

SCIENTIFIC REPORTS



OPEN

Physics of transportation: Towards optimal capacity using the multilayer network framework

Wen-Bo Du¹, Xing-Lian Zhou¹, Marko Jusup² & Zhen Wang³

Received: 08 October 2015
Accepted: 02 December 2015
Published: 21 January 2016

Because of the critical role of transportation in modern times, one of the most successful application areas of statistical physics of complex networks is the study of traffic dynamics. However, the vast majority of works treat transportation networks as an isolated system, which is inconsistent with the fact that many complex networks are interrelated in a nontrivial way. To mimic a realistic scenario, we use the framework of multilayer networks to construct a two-layered traffic model, whereby the upper layer provides higher transport speed than the lower layer. Moreover, passengers are guided to travel along the path of minimal travelling time and with the additional cost they can transfer from one layer to another to avoid congestion and/or reach the final destination faster. By means of numerical simulations, we show that a degree distribution-based strategy, although facilitating the cooperation between both layers, can be further improved by enhancing the critical generating rate of passengers using a particle swarm optimisation (PSO) algorithm. If initialised with the prior knowledge from the degree distribution-based strategy, the PSO algorithm converges considerably faster. Our work exemplifies how statistical physics of complex networks can positively affect daily life.

Statistical physics of complex networks¹, due to broad applicability, has served as the analytical foundation for the analysis of many problems related to the modern infrastructure^{2–6}. Physics of transportation in particular received a lot of attention^{7–13}, which may not come as a surprise given the increasingly severe traffic congestion around the world. For achieving a higher capacity, it was shown that both the network structure and the routing strategy are of major importance when designing vital transportation infrastructure^{14–19}. Accordingly, the number of routing algorithms based on physical methods has swelled over the years, where some of the better known examples include global dynamic routing¹⁶, degree-driven delivering strategy¹⁷, betweenness related edge deletion¹⁸, traffic-awareness strategy^{20,21}, adaptive routing strategy²², and the optimal local routing strategy²³, to name a few.

Despite all the interest in physics of transportation, a prevailing assumption has been that the nodes of a network have a single degree distribution and therefore interact in a manner described by a single network layer. In reality, however, most transportation systems are composed of many interconnected networks, thus representing a typical problem for which statistical physicists devised the multilayer network framework^{24–31}. Within such a framework, many interesting dynamical phenomena may arise. One of the best known examples is a cascading failure of interdependent networks, whereby seemingly irrelevant alterations in one network have unexpected and catastrophic consequences for the other²⁴. Thereafter, physicists in collaboration with scientists from related disciplines examined the multilayer network structure in the context of (i) assortativity and the robustness against attacks³², (ii) inter-similarity and cascading failure³³, (iii) diffusion³⁴, (iv) disease spreading and prevention³⁵, (v) evolutionary games^{36,37}, (vi) voting³⁸, and (vii) synchronisation³⁹. In some instances, physics of transportation either motivated or was the direct target of research based on multilayer networks^{40,41}. A particularly nice example are interrelated networks of airports and seaports such that, in a given city, the functioning of the city's airport is dependent upon resources coming from the seaport and vice versa⁴².

The multilayer framework, as it appeared in statistical physics of complex networks, promises to describe traffic dynamics beyond what is possible using more traditional isolated networks. By representing physical

¹School of Electronic and Information Engineering, Beihang University, Beijing 100191, P.R.China. ²Faculty of Sciences, Kyushu University, Fukuoka 819-0395, Japan. ³Interdisciplinary Graduate School of Engineering Sciences, Kyushu University, Fukuoka 816-8580, Japan. Correspondence and requests for materials should be addressed to W.-B.D. (email: wenbodu@buaa.edu.cn) or M.J. (email: mjusup@gmail.com) or Z.W. (email: zhenwang0@gmail.com)

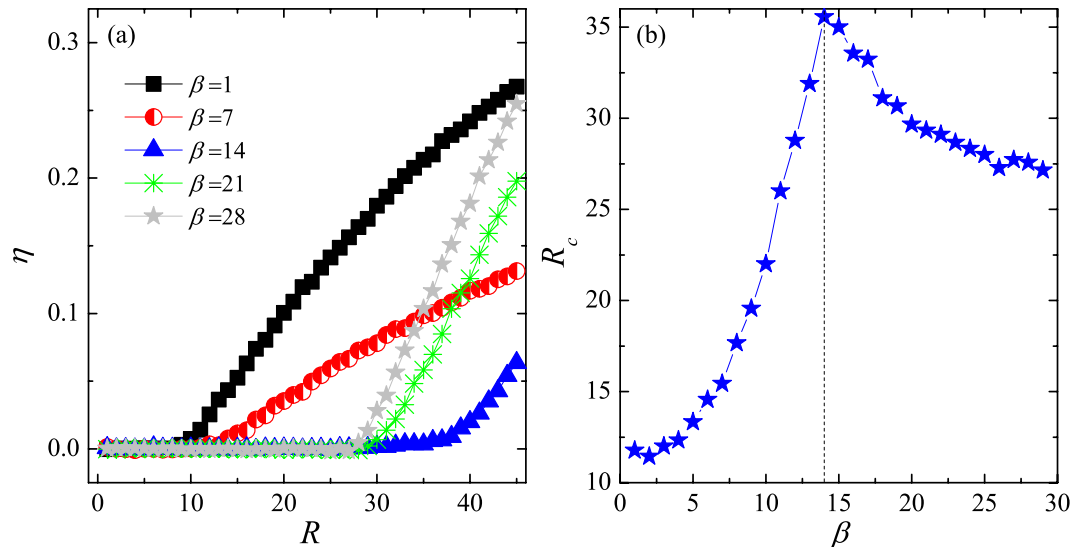


Figure 1. System's performance under an even transfer-cost allocation. (a) Order parameter η as a function of generating rate R at several values of transfer cost β . (b) Critical generating rate R_c as a function of β . Maximum R_c corresponds to $\beta = 14$ marked by the dashed line. The results are averaged over 30 independent realisations.

infrastructure as one network layer and traffic flows as another, ref. 31 found some fundamental differences between the load estimators and the real load. Furthermore, a model of layered transportation in ref. 27 led to the introduction of the cooperation strength as an order parameter and revealed a phase transition at the onset of cooperation. The order parameter changed from zero to positive at the transition point. Finally, the results of ref. 28 indicated that coupled spatial systems may cause behaviour dependent on the interplay between the coupling and the source-sink distribution. Inspired by these discoveries, we use a two-layered network model to optimise the capacity of a predetermined infrastructure, where a central role is played by transfer costs incurred when passengers switch between the coupled networks. We show that an optimised allocation of transfer costs is achievable using a particle swarm optimisation (PSO) algorithm to increase the total capacity of the infrastructure.

Results

We start the analysis of the model described in the Methods section from the simplest possible case—a constant transfer cost, β , at all coupled nodes (i.e. $\beta_p = \beta$, where p indexes a unique node). Let us denote by R the number of new passengers that enter the system at each time step t . Source and destination locations of passengers are assigned randomly. Furthermore, nodes are assumed to have the capacity to deliver C passengers in a single time step. One of the most important properties of a transportation system is the balance between passenger handling and delivering capacities, which is appropriately captured by the critical generating rate, R_c , at which a continuous phase transition takes place from a free-flow to a congested state. To describe such a critical phenomenon, we consider an order parameter, $\eta^{14,43}$, defined as

$$\eta = \lim_{t \rightarrow \infty} \frac{C \langle \Delta w \rangle}{R \Delta t}, \quad (1)$$

where $\Delta w = w(t + \Delta t) - w(t)$, with $w(t)$ being the total number of passengers in the system at time step t , and $\langle \cdot \rangle$ the averaging operator over time windows of width Δt . In a free-flow state (i.e. $R < R_c$), the balance between generated and removed traffic guarantees $\eta = 0$. By contrast, a congested state (i.e. $R > R_c$) occurs if the number of accumulated passengers increases with time, thus causing $\eta > 0$. Figure 1(a) shows order parameter η as a function of R at different values of the transfer cost, β . We see that $\eta = 0$ when R is small irrespective of the value of β , but begins to increase monotonously when R reaches the critical point, R_c . Moreover, because the transition happens at different critical points, the network capacity varies with β . An interesting question thus poses itself; what value of the transfer cost, β , maximises the system's capacity?

The simulation results in Fig. 1(b) show that $\beta = 14$ maximises the critical threshold R_c . If the transfer cost is low (e.g. $\beta = 1$), passengers prefer to travel in the upper layer due to its high speed, but can easily return to the lower layer to reach their final destinations—a form of cooperation establishes itself between the two layers. However, as passengers enter the system at a higher and higher rate, the upper layer reaches a congestion state, which in turn causes a system-wide traffic jam. The system's capacity is thus close to the capacity of the upper layer. By contrast, if the transfer cost is excessive (e.g. $\beta = 29$), most passengers choose to stay only in one layer—it becomes more difficult to establish the same form of cooperation as before. Because the lower layer has a greater capacity, the total system's capacity approaches that of the lower layer. Between these extremes (e.g. $\beta = 14$), high speed and extra transfer costs are well-balanced to produce the optimal capacity of the system.

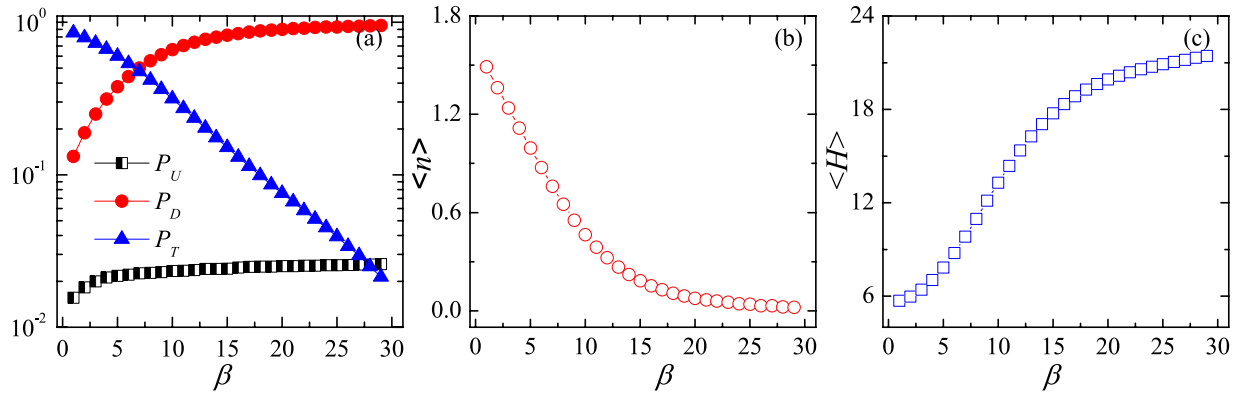


Figure 2. How the optimal capacity arises? (a) Traffic flows P_U , P_D , and P_T , (b) the average number of transfers, $\langle n \rangle$, and (c) the average number of hops, $\langle H \rangle$, all presented as the functions of transfer cost β .

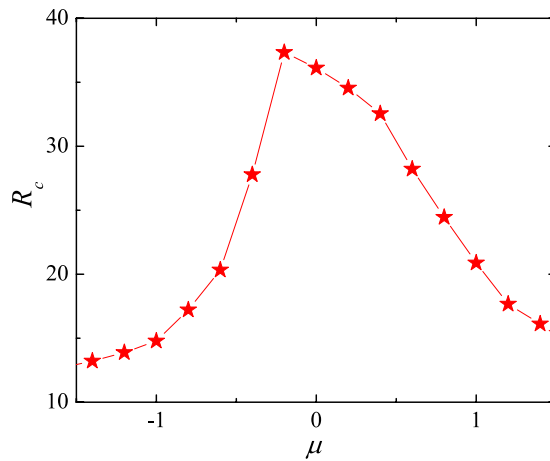


Figure 3. Optimising the system’s capacity under a biased transfer-cost allocation. Critical generating rate R_c as a function of parameter μ at $S = 2800$ (corresponding to $\beta = 14$).

To better understand how the optimal capacity arises, we investigate the dependence of the travel behaviour of passengers on the transfer cost. Specifically, the traffic flow is subdivided into three types: the flow in the upper layer, P_U , the flow in the lower layer, P_D , and the flow of passengers transferring from one layer to another, P_T . As shown in Fig. 2(a), P_T decreases, while P_U and P_D increase with β , thus indicating that passengers are more bound to a layer where they entered the system when the cost is high. This result is further confirmed by the average number of transfers $\langle n \rangle$, which monotonously decreases with β as shown in Fig. 2(b). A higher transfer cost, therefore, suppresses the cooperation between the two layers. Suppressed cooperation diminishes the opportunities for exploiting more direct routes in the upper layer and hence passengers have to endure stopping at more stations, which is indicated in Fig. 2(c) by the average number of hops along the way, $\langle H \rangle$. When the system is functioning at the maximum capacity (i.e. $\beta = 14$), we have $\langle n \rangle \approx 0.223$ and $\langle H \rangle \approx 17.1$, suggesting more reliance on the lower layer with only a limited number of passengers transferring between layers to alleviate congestion.

Thus far, we explored the simplest assumption of an even distribution of the transfer cost (i.e. $\beta_p = \beta$ for all p), whereas in reality the transfer cost may have different values in each coupled node. Inspired by the knowledge that the optimal capacity is often related with degree centrality or betweenness centrality^{14,17}, we introduce a new transfer cost as:

$$\beta_p = \frac{k_p^\mu}{\sum_p^{N_U} k_p^\mu} * S, \tag{2}$$

where k_p is the degree of coupled node p in the upper layer, $S = \beta * N_U$ is the total cost of transfers N_U is the number of nodes in the upper layer, and μ is an adjustable parameter. If $\mu = 0$, we recover the above-studied case of an even transfer-cost allocation (hereafter “EFA”); otherwise the allocation is biased (“BFA”).

In analysing the BFA, we first explore if there exists a particular value of μ that maximises the system’s capacity at fixed β . In Fig. 3, the critical point, R_c , is shown as a function of μ , where $S = 2800$ to maintain $\beta = 14$ from Fig. 1(b). The maximum value of R_c , and hence the optimal capacity, is indeed reached at $\mu = -0.2$. Yet, when β changes, Fig. 4 indicates that reaching the maximum capacity requires μ to change as well. The failure to find

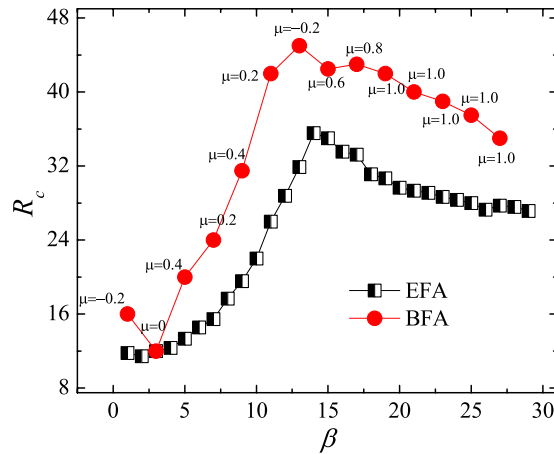


Figure 4. Comparing the two transfer-cost allocations (EFA and BFA). Critical generating rate R_c as a function of transfer cost β . The optimal value of parameter μ changes with β .

a single best value of μ seems to be pointing to the conclusion that the allocation of transfer costs according to degree centrality may not be the best strategy.

If degree centrality is not the best strategy, can we find a better transfer-cost allocation that would make the system's capacity higher? The problem can formally be written as

$$\max R_c(\vec{\beta}) \text{ s.t. } \begin{cases} g(\vec{\beta}) \leq S \\ \beta_p \geq 0, \text{ for all } p \end{cases}$$

where $g(\vec{\beta}) \leq S$ is the inequality constraint, with $\vec{\beta}$ being a short-hand notation for a vector comprised of components β_p , $p = 1, \dots, N_U$. We set $g(\vec{\beta}) = \sum_p \beta_p$ to define an upper limit, S , for the total transfer cost. The critical generating rate of passengers, $R_c(\vec{\beta})$, is in the context of optimisation called the objective function. Vector $\vec{\beta}$ that maximises the objective function and satisfies the above-defined inequality constraint and variable bounds is called a feasible solution; otherwise the solution is infeasible.

Because the objective function, $R_c(\vec{\beta})$, is nonlinear and without an analytical expression in the case of coupled networks, we resort to intelligent computing to solve the optimisation problem at hand. Specifically, we employ the particle swarm optimisation (PSO) algorithm⁴⁴, a technique inspired by the social behaviour of swarms⁴⁵ and widely used to solve a number of optimisation problems^{46–50}. The PSO algorithm with constraint handling used herein searches for a solution while obeying the following rules:

- (1) The objective function is redefined and separated into two parts: the fitness function, $F(\vec{\beta})$, and the constraint violation function, $V(\vec{\beta})$, where $F(\vec{\beta}) = R_c(\vec{\beta})$ and $V(\vec{\beta}) = 0$ if $g(\vec{\beta}) \leq S$; otherwise $V(\vec{\beta}) = g(\vec{\beta}) - S$.
- (2) A pair-wise comparison of candidate solutions is performed in such a way that:
 - (a) when two feasible solutions are compared, the one with higher fitness is chosen;
 - (b) when two infeasible solutions are compared, the one with lower constraint violation is chosen;
 - (c) when a feasible and an infeasible solutions are compared, the infeasible solution is chosen only if it has higher fitness and the constraint violation is less than $\varepsilon > 0$; otherwise the feasible solution is chosen.

As a result of these rules, the PSO algorithm may choose an infeasible solution as the optimum, but such a solution is guaranteed to be near the boundary of the set of feasible solutions.

Next, we examine the performance of our toy-model transportation system after optimisation with the PSO algorithm. Figure 5 displays the order parameter, η , as a function of the passenger generating rate, R , under different transfer-cost allocation methods. The PSO algorithm considerably increases the critical point, R_c , relative to EFA and BFA methods, thus clearly outperforming them. A drawback of the PSO algorithm is a lengthy computation time, especially if the algorithm is initialised randomly. From Fig. 3, we know that the maximum R_c is obtained for $\beta = 14$ and $\mu = -0.2$, so it seems reasonable to use such prior knowledge during initialisation to decrease the computation time. Figure 6 compares the performance of the PSO algorithm under the two initialisation options. If the prior knowledge is used, the PSO algorithm converges faster and is able to find a better solution (i.e. higher R_c) within the preset number of iterations. We, therefore, discuss the properties of the optimised transportation system only in the case of initialisation with the prior knowledge.

A closer look at the performance of the PSO algorithm as a function of the (Euclidean) distance, $\langle D \rangle$, between departure and destination nodes reveals several interesting outcomes. Here, as in refs 51,52, the variance of the travelling time, δ_T , is used as an intuitive reliability indicator because it is highly undesirable for some passengers to be stuck, while others progress smoothly through the system. Figure 7(a) shows that the PSO algorithm controls δ_T much better than EFA or BFA methods, indicating that the optimised system functions more reliably.

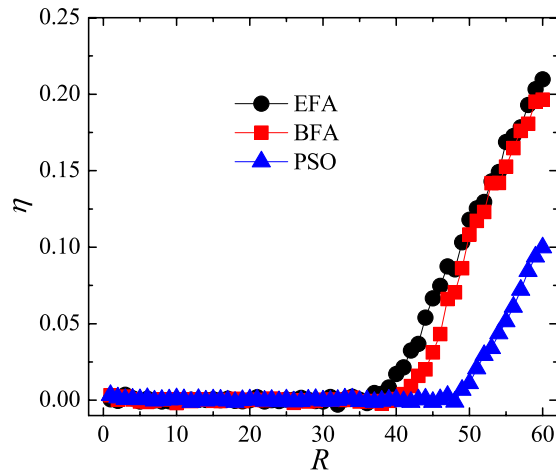


Figure 5. Particle swarm optimisation increases the system's capacity. Order parameter η as a function of generating rate R under the three transfer-cost allocations (EFA, BFA, and PSO).

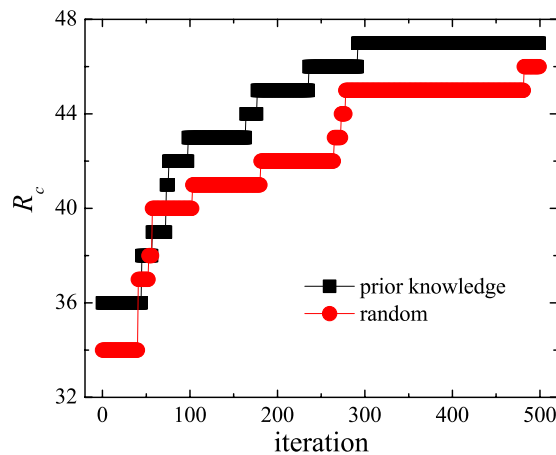


Figure 6. Improving the performance of the PSO algorithm. Critical generating rate R_c as a function of the number of iterations under the two initialisation methods (random and prior knowledge).

Furthermore, in Fig. 7(b) the average cost of traversed paths, $\langle L \rangle$, is lower if the system is optimised using the PSO algorithm instead of EFA or BFA methods. The last result, to be precise, holds only if $\langle D \rangle$ is higher than 15, but mid- to long-distance journeys are the ones where cutting costs makes the most economic and ecological sense (e.g. by considerably reducing the fuel consumption). Finally, Fig. 7(c) shows that in the interval $\langle D \rangle \in [20, 35]$ the PSO algorithm generates the highest average number of transfers, $\langle n \rangle$, of the three methods. Optimised systems, therefore, are more reliant on transferring passengers who travel mid to long distances in order to alleviate congestion.

Conclusion

Using ideas and concepts from statistical physics of complex networks, particularly the multilayer network framework, we built a two-layered idealised transportation system and examined the implied dynamics. Each layer had a different topology and supported different travelling speed—characteristics that qualitatively correspond to real-life transportation systems. Seeking to minimise the travelling time of passengers, we allowed transfers between the two layers at an extra cost with the purpose of (i) taking the advantage of high speed offered by the upper layer or (ii) reaching a final destination served only by the, in relative terms slow, lower layer.

Our main concern was the influence of transfer costs on the transportation system's capacity. We found that an even transfer-cost allocation (EFA) maximises the system's capacity by fine-tuning the trade-off between high speed and extra transfer costs. Somewhat at odds with the general consensus reached by examining traffic dynamics in isolated networks, a degree centrality-based strategy (BFA) was not overly helpful in enhancing the performance of the system. However, starting from such a strategy and reassigning transfer costs using a particle swarm optimisation (PSO) algorithm improved the capacity and several other properties of the system at a reasonable computational cost. Our work exemplifies how statistical physics of complex networks can positively affect daily life.

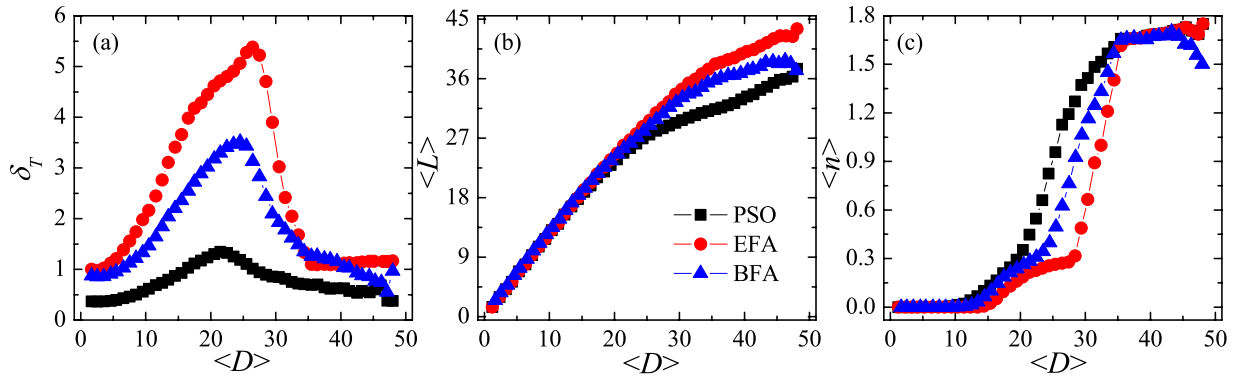


Figure 7. Performance of the optimised system. (a) The variance of the travelling time, δ_T , (b) the average cost of traversed paths, $\langle L \rangle$, and (c) the average number of transfers, $\langle n \rangle$, as functions of average distance $\langle D \rangle$ between departure and destination nodes. The generating rate is $R = 60$.

Finally, a word of caution regarding the optimality of the solution is in order. When considering real-world optimisation problems, it is often hard, if not impossible, to obtain a theoretical optimal solution. Therefore, it is quite common to rely on heuristic optimisation—such as the genetic algorithm, differential evolution, and PSO—although none of these methods guarantees an optimal solution. What heuristic optimisation usually does is improving upon a solution suggested by experts. Herein, for example, we combine the commonly used and well-documented PSO algorithm with a strategy suggested by the system’s topology in order to allocate transfer costs “optimally”. The main contribution thus is precisely the fact that we *can* find an optimisation-based strategy that is better than the topology-based (i.e. “expert”) strategy. We stayed clear of comparing the current best solution with the best solutions that other algorithms may have generated, the reason being that such a comparison is perhaps more interesting to the readers of journals specialised in intelligent computing. Nevertheless, it is an interesting topic for future research.

Methods

Here, we consider a toy model that exhibits the same main characteristics as many modern transportation systems composed of, for example, a train and an aeroplane network. The model employs a two-layer architecture: the lower layer is a von Neumann-neighbourhood lattice containing $N_D \times N_D$ nodes⁵³, whereas the upper layer, constructed using the scale-free algorithm⁵⁴, has N_U nodes with the average degree $\langle k \rangle = 12$. The transport speed in each network is different. Without any loss of generality, we work in units in which the speed of the lower layer is $V_D = 1$ and the speed of the upper layer is $V_U = \alpha \times V_D$, where we fix $\alpha = 3$ as the realistic speed ratio between aeroplane and high-speed railway networks. To make transfers between the two layers possible, each node in the upper layer is connected to one randomly selected counterpart from the lower layer (i.e. there are N_U coupled nodes). For the purpose of calculating distances, nodes in the upper layer are assigned the same coordinates as their counterparts from the lower layer. Furthermore, the taxicab metric is used in the lower layer, where the length of an edge connecting two neighbours is $D_{ij} = 1$. In the upper layer, by contrast, the distance between two neighbours is given by the Euclidean metric, $U_{ij} = \sqrt{(x_i - x_j)^2 + (y_i - y_j)^2}$, where (x_i, y_i) are the coordinates of node i . For simplicity, we mainly focus on two layers with $N_D = 200$ and $N_U = 35$. Enlarging both networks by the same factor guarantees the same quantitative observations.

After defining the underlying infrastructure, the transport process is carried out as follows. At each time step, t , a number of new passengers, R , with random sources and destinations are assigned to the system of networks. Each node has the capacity to deliver C passengers in one time step (we set $C = 1$ in simulations), complemented with an infinite queue buffer to handle the congestion. Passengers in the system are navigated in the way that minimises their travelling time. The primary purpose of transfers is to reduce the total time of travel, which comes at an economic cost. Generally, a passenger is willing to pay a certain number of monetary units for a given time reduction, thus allowing us to express the transfer cost, β_p , at coupled node p in units of time. With these definitions, passengers between any two nodes i and j are delivered along such a path, $P_{i \rightarrow j} = \{i \equiv X_0, X_1, \dots, X_{n-1}, X_n \equiv j\}$, that minimises the quantity

$$L(P_{i \rightarrow j}) = \min \left(\sum_{m=0}^{n-1} t(X_m, X_{m+1}) + \sum_p \beta_p \right) \quad (3)$$

where the first term in brackets is the total time of travel, given here as the sum of individual travelling times $t(X_m, X_{m+1})$ between the two successive nodes, X_m and X_{m+1} , along path $P_{i \rightarrow j}$ calculated as the ratio of speed to distance. The second term, $\sum_p \beta_p$, represents the total transfer cost. When a passenger reaches the destination, it is removed from the system. Note that quantity L can be interpreted as the total cost in units of time associated with path $P_{i \rightarrow j}$.

The PSO algorithm is usually specified by three parameters. We denote these parameters with c_1 , c_2 , and η . The values are $c_1 = c_2 = 2.05$ and $\eta = 0.7298$. The number of particles is 20 and the number of iterations 300.

References

- Albert, R. & Barabási, A. L. Statistical mechanics of complex networks. *Rev. Mod. Phys.* **74**, 47 (2002).
- Rinaldi, S. M., Peerenboom, J. P. & Kelly, T. K. Identifying, understanding, and analyzing critical infrastructure interdependencies. *IEEE Contr. Syst. Magn.* **21**, 11–25 (2001).
- Rosato, V. *et al.* Modelling interdependent infrastructures using interacting dynamical models. *Int. J. Crit. Infrastruct.* **4**, 63–79 (2008).
- Panzieri, S. & Setola, R. Failures propagation in critical interdependent infrastructures. *Int. J. Model. Ident. Contr.* **3**, 69–78 (2008).
- Gao, Z. K. *et al.* Multivariate weighted complex network analysis for characterizing nonlinear dynamic behavior in two-phase flow. *Exp. Therm. Fluid Sci.* **60**, 157–164 (2015).
- Gao, Z. K. *et al.* Multi-frequency complex network from time series for uncovering oil-water flow structure. *Sci. Rep.* **5**, 8222 (2015).
- Barrat, A., Barthélemy, M., Pastor-Satorras, R. & Vespignani, A. The architecture of complex weighted networks. *Int. J. Model. Ident. Contr.* **101**, 3747 (2004).
- Guimerà, R., Mossa, S., Turtschi, A. & Amaral, L. A. N. The world-wide air transportation network: anomalous centrality, community structure, and cities global roles. *Proc. Natl. Acad. Sci. USA* **102**, 7794–7799 (2005).
- Yang, H. *et al.* Scaling properties in spatial networks and their effects on topology and traffic dynamics. *EPL* **89**, 613–630 (2010).
- Sen, P. *et al.* Small-world properties of the Indian railway network. *Phys. Rev. E* **67**, 036106 (2003).
- Seaton, K. A. & Hackett, L. M. Stations, trains and small-world networks. *Physica A* **339**, 635–644 (2004).
- Cardillo, A., Scellato, S., Latora, V. & Porta, S. Structural properties of urban street patterns, discovering the backbone of a city. *Eur. Phys. J. B* **50**, 221–225 (2006).
- Barthélemy, M. & Flammini, A. Modeling urban street patterns. *Phys. Rev. Lett.* **100**, 13 (2008).
- Wang, W. X. *et al.* Traffic dynamics based on local routing protocol on a scale-free network. *Phys. Rev. E* **73**, 026111 (2006).
- Huang, W. & Chow, T. W. S. Effective strategy of adding nodes and links for maximizing the traffic capacity of scale-free network. *J. Stat. Mech.* **20**, 233–271 (2010).
- Ling, X., Hu, M.-B., Jiang, R. & Wu, Q. S. Global Dynamic Routing for Scale-free Networks. *Phys. Rev. E* **81**, 132–135 (2010).
- Yan, G., Zhou, T., Hu, B., Fu, Z. Q. & Wang, B. H. Efficient routing on complex networks. *Phys. Rev. E* **73**, 046108 (2006).
- Zhang, G. Q., Wang, D. & Li, G. J. Enhancing the transmission efficiency by edge deletion in scale-free networks. *Phys. Rev. E* **76**, 017101 (2007).
- Zhao, L., Park, K. & Lai, Y. C. Attack vulnerability of scale-free networks due to cascading breakdown. *Phys. Rev. E* **70**, 035101 (2004).
- Echenique, P., Gómez-Gardeñes, J. & Moreno, Y. Improved routing strategies for Internet traffic delivery. *Phys. Rev. E* **70**, 056105 (2004).
- Echenique, P., Gómez-Gardeñes, J. & Moreno, Y. Dynamics of jamming transitions in complex networks. *EPL* **71**, 823–829 (2005).
- Zhang, H., Liu, Z., Tang, M. & Hui, P. M. An adaptive routing strategy for packet delivery in complex networks. *Phys. Lett. A* **364**, 177–182 (2007).
- Li, K., Gong, X., Guan, S. & Lai, C. H. Analysis of traffic flow on complex networks. *Internat. J. Modern Phys. B* **25**, 1419 (2011).
- Buldyrev, S. V., Parshani, R., Paul, G., Stanley, H. E. & Havlin, S. Catastrophic cascade of failures in interdependent networks. *Nature* **464**, 1025–1028 (2010).
- Anna, S. M., Mángeles, S. & Marián, B. (2012). Epidemic spreading on interconnected networks. *Phys. Rev. E* **86**, 1818–1834 (2012).
- Hu, Y. *et al.* Percolation of interdependent networks with intersimilarity. *Phys. Rev. E* **88**, 052805 (2013).
- Gu, C. G. *et al.* Onset of cooperation between layered networks. *Phys. Rev. E* **84**, 1465–1474 (2011).
- Morris, R. G. & Barthelemy, M. Transport on coupled spatial networks. *Phys. Rev. Lett.* **109**, 128703 (2012).
- Hu, Y., Havlin, S. & Makse, H. A. Conditions for viral influence spreading through multiplex correlated social networks. *Phys. Rev. X* **4**, 021031 (2014).
- Boccaletti, S. *et al.* The structure and dynamics of multilayer networks. *Phys. Rep.* **544**, 1C122 (2014).
- Kurant, M. & Thiran, P. Layered Complex Networks. *Phys. Rev. Lett.* **96**, 138701 (2006).
- Tan, F., Xia, Y., Zhang, W. & Jin, X. (2013). Cascading failures of loads in interconnected networks under intentional attack. *EPL* **102**, 28009 (2013).
- Hu, Y. *et al.* Percolation of interdependent networks with intersimilarity. *Phys. Rev. E* **88**, 4482–4498 (2013).
- Gómez, S. *et al.* Diffusion dynamics on multiplex networks. *Phys. Rev. Lett.* **110**, 1154–1154 (2013).
- Funk, S., Gilad, E., Watkins, C. & Jansen, V. A. The spread of awareness and its impact on epidemic outbreaks. *Proc. Natl. Acad. Sci. USA* **106**, 6872–6877 (2009).
- Wang, Z., Szolnoki, A. & Perc, M. Interdependent network reciprocity in evolutionary games. *Sci. Rep.* **3**, 1183 (2013).
- Wang, Z., Wang, L., Szolnoki, A. & Perc, M. Evolutionary games on multilayer networks: a colloquium. *Eur. Phys. J. B* **88**, 1–15 (2015).
- Mucha, P. J. & Porter, M. A. Communities in multislice voting networks. *Chaos* **20**, 701–706 (2010).
- Porfiri, M. & Bernardo, M. D. Criteria for global pinning-controllability of complex networks. *Automatica* **44**, 3100–3106 (2008).
- Tan, F., Wu, J., Xia, Y. & Tse, K. T. Traffic congestion in interconnected complex networks. *Phys. Rev. E* **89**, 062813 (2014).
- Zhuo, Y., Peng, Y., Liu, C., Liu, Y. & Long, K. Traffic dynamics on layered complex networks. *Physica A* **390**, 2401C2407 (2011).
- Parshani, R., Rozenblat, C., Letri, D., Ducruet, C. & Havlin, S. Inter-similarity between coupled networks. *EPL* **92**, 68002 (2010).
- Arenas, A., Díaz-Guilera, A. & Guimerà, R. Communication in networks with hierarchical branching. *Phys. Rev. Lett.* **86**, 3196–3199 (2000).
- Kennedy, J. & Eberhart, R. Particle Swarm Optimization. *Proceedings of the International Conference on Neural Networks* 1942 (1995).
- Vicsek, T., Czirók, A., Ben-Jacob, E., Cohen, I. I. & Shochet, O. Novel type of phase transition in a system of self-driven particles. *Phys. Rev. Lett.* **75**, 1226–1229 (1995).
- Easter, S. *et al.* Parameter estimation in stochastic mammogram model by heuristic optimization techniques. *IEEE Trans. Inf. Technol. B* **10**, 685–695 (2006).
- Gaing, Z. L. & Gaing, Z. L. Particle swarm optimization to solving the economic dispatch considering the generator constraints. *IEEE Trans. Power Sys.* **18**, 1187–1195 (2003).
- Du, W. B., Gao, Y., Liu, C., Zheng, Z. & Wang, Z. Adequate is better: particle swarm optimization with limited-information. *Appl. Math. and Comp.* **268**, 832C838 (2015).
- Gao, Y., Du, W. & Yan, G. electively-informed particle swarm optimization. *Sci. Rep.* **5**, 9295 (2015).
- Liu, C., Du, W. B. & Wang, W. X. Particle Swarm Optimization with Scale-free Interactions. *PLoS One* **9**, e97822 (2014).
- Hong, K. L. & Tung, Y. K. Network with degradable links: capacity analysis and design. *Transport. Res. B* **37**, 345–363 (2003).
- Lo, H. K. A reliability framework for traffic signal control. *IEEE Trans. Intell. Transp. Syst.* **7**, 250–260 (2006).
- Du, W. B., Zhou, X. L., Chen, Z., Cai, K. Q. & Cao, X. B. Traffic dynamics on coupled spatial networks. *Chaos, Solitons & Fractals* **68**, 72C77 (2014).
- Barabási, A. L. & Albert R. Emergence of Scaling in Random Networks. *Science* **286**, 509 (1999).

Acknowledgements

This work was supported by (i) the National Basic Research Program of China (Grant no. 2011CB707000), (ii) the National Natural Science Foundation of China (Grant no. 61201314 and 60921001), (iii) National Key Technology R&D Program of China (Grant no. 2012BAG04B01), and (iv) Japan Society for the Promotion of Science (JSPS) Postdoctoral Fellowship Program for Foreign Researchers (no. P13380) and an accompanying Grant-in-Aid for Scientific Research.

Author Contributions

W.-B.D., X.-L.Z., M.J. and Z.W. planned the study, performed the simulations, analyzed the results, and wrote the paper.

Additional Information

Competing financial interests: The authors declare no competing financial interests.

How to cite this article: Du, W.-B. *et al.* Physics of transportation: Towards optimal capacity using the multilayer network framework. *Sci. Rep.* **6**, 19059; doi: 10.1038/srep19059 (2016).



This work is licensed under a Creative Commons Attribution 4.0 International License. The images or other third party material in this article are included in the article's Creative Commons license, unless indicated otherwise in the credit line; if the material is not included under the Creative Commons license, users will need to obtain permission from the license holder to reproduce the material. To view a copy of this license, visit <http://creativecommons.org/licenses/by/4.0/>